Electronic Supplementary Material (ESI) for Dalton Transactions.
This journal is © The Royal Society of Chemistry 2024

Origin of the Cr^{3+} concentration-dependent broadband near-infrared emission in $Sc_2Si_2O_7$

Siyuan Xie, Boxin Ma, Dawei Wen, Qingguang Zeng, Yue Guo*, Ting Yu*

School of Applied Physics and Materials, Wuyi University, Jiangmen, Guang dong, 529020, P. R. China

* *Email: guoyuewyu@163.com, yuting1009@163.com*

1. Materials synthesis

A series of Cr^{3+}-activated $Sc_{2-x}Si_2O_7$:xCr^{3+} (x = 0.001, 0.003, 0.005, 0.01, 0.02, 0.05, 0.07, 0.10) phosphors were synthesized by a traditional high-temperature solid-state reaction method. Sc_2O_3 (99.99%), SiO_2 (99.99%), and Cr_2O_3 (99.95%) were used as raw materials without further purification. The raw materials were mixed in an agate mortar according to the stoichiometric ratio and finely ground with an appropriate amount of anhydrous ethanol for 30 mins. The mixture was transferred to an alumina crucible and sintered at 1600 °C for 4 h in tube furnace under a reducing atmosphere of 20%H_2+80%N_2. After cooling to room temperature, the $Sc_{2x}Si_2O_7$:xCr^{3+} phosphors were reground into powder for further characterization.

2. Characterization

The phase purity and crystal structure of $Sc_{2-x}Si_2O_7$:xCr^{3+} samples were checked by a PanAnalytical X'Pert powder diffractometer (XRD) operating with Cu Kα radiation source (λ = 1.5405 Å) under 40 kV and 40 mA at room temperature (2θ range of 15º-70º). High-quality X-ray diffraction (XRD) data for Rietveld refinement were obtained from the above instrument ranging from 10° to 130° with a step size of 0.008°. The Rietveld refinement employed the general structure analysis system (GSAS-II) software suite.[1] The morphology of the as-obtained phosphors and energy-disperse X-ray spectroscopy (EDS) were visualized on a field-emission scanning electron microscope (SEM, Zeiss Sigma 500). Ultraviolet-Visible diffuse reflection spectra (UV-Vis DRS) were measured on a Shimadzu UV-3600 plus UV–Visible–NIR spectrophotometer with $BaSO_4$ powder as a reflectance standard. The photoluminescence excitation spectra (PLE) and emission spectra (PL) were recorded by an Edinburgh Instruments FLS980 fluorescence spectrometer with a 450 W Xe

lamp as the excitation source and a liquid nitrogen-cooled Hamamatsu R5509-72 PMT for the detection of NIR emission. The PL decay curves were collected by an Edinburgh Instruments FLS980 fluorescence spectrometer with a microsecond μF900 xenon lamp as the pulsed excitation source. The electron spin resonance spectra (EPR) were taken on a Bruker EMXnano. The chemical states of the Cr were performed by X-ray photoelectron spectrometer (XPS, Thermo SCIENTIFIC Nexsa) with an Al anode (Al-Kα= 1486.68 eV) as X-ray source.

Table S1. The main refinement parameters of $Sc_2Si_2O_7$ and $Sc_{1.95}Si_2O_7$:0.05Cr^{3+}

Formula	$Sc_2Si_2O_7$	$Sc_{1.95}Si_2O_7$:0.05Cr^{3+}
Space group	$C2/m$	
a (Å)	6.5049(3)	6.49615(22)
b (Å)	8.50090(9)	8.49426(6)
c (Å)	4.67981(17)	4.67487(12)
$\alpha=\gamma$ (°)	90	90
β (°)	102.7905(9)	102.7109(6)
Volume(Å^3)	252.3615(31)	251.6375(21)
R_p (%)	6.09	5.84
R_{wp} (%)	8.69	7.96
GOF	3.17	2.88

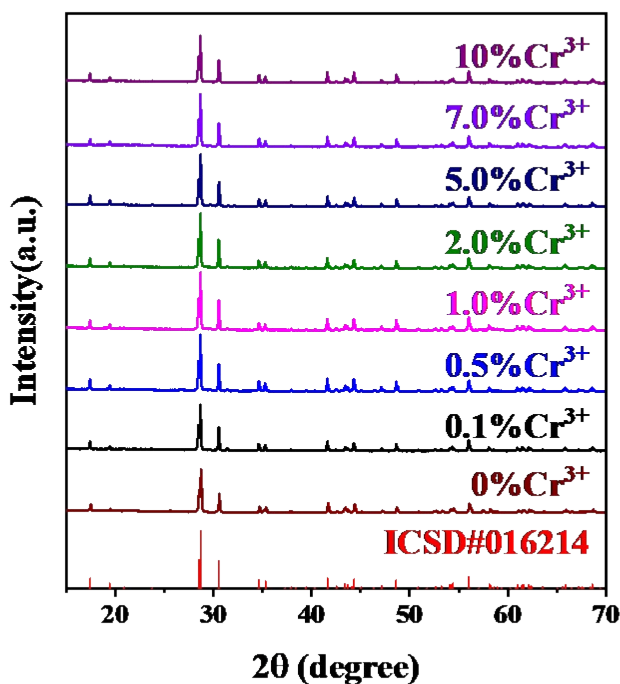

Fig. S1 XRD patterns of $Sc_{2-x}Si_2O_7$:xCr^{3+} (x =0 -0.1).

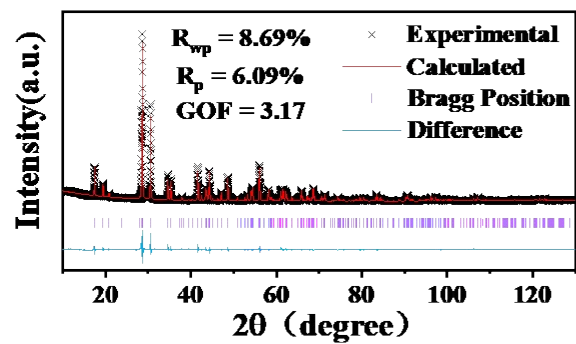

Fig. S2 XRD refinements of $Sc_2Si_2O_7$.

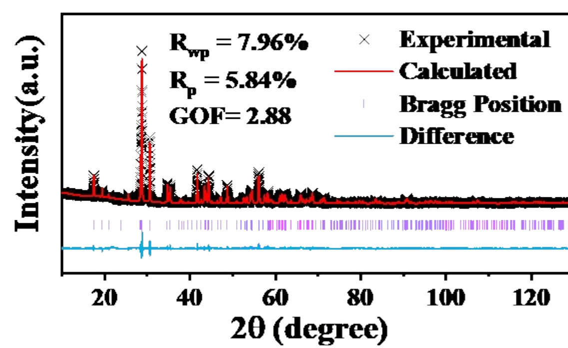

Fig. S3 XRD refinements of $Sc_{1.95}Si_2O_7$:$0.05Cr^{3+}$.

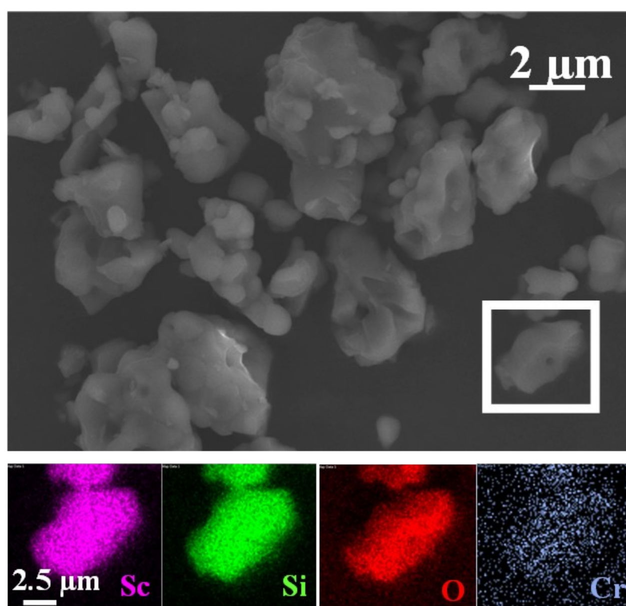

Fig. S4 SEM images and EDS elemental mapping images of $Sc_{1.95}Si_2O_7$:$0.05Cr^{3+}$.

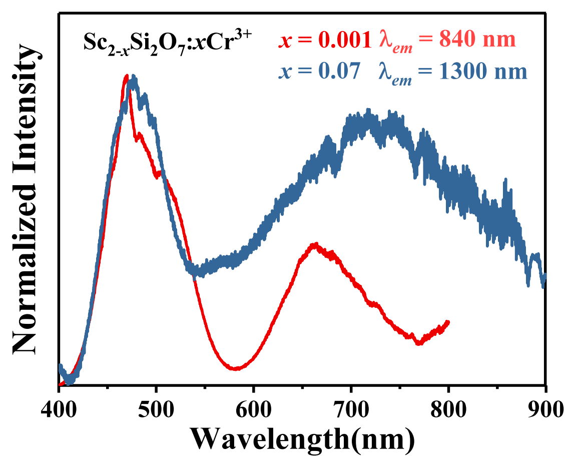

Fig. S5 Normalized PLE (λem = 840 nm and 1300nm) spectra.

PLE spectrum of two luminescent centers located at 840 nm and at 1300 nm, respectively. Although the shape of the PLE spectrum at 1300 nm is similar to that at 840 nm, it is slightly shifted at 600-900 nm.

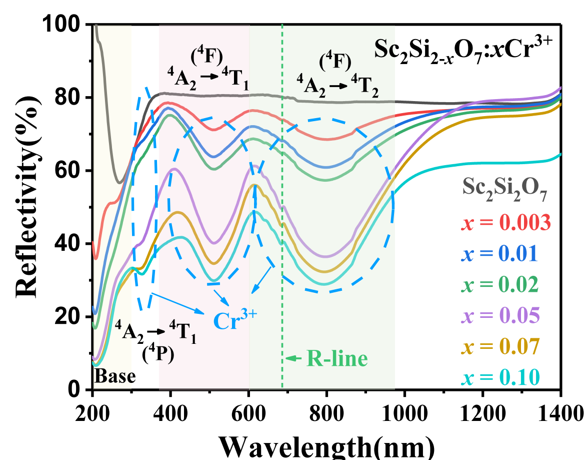

Fig. S6 UV-Vis–NIR DRS of $Sc_{2\text{-}x}Si_2O_7$:$x$$Cr^{3+}$.

The absorption peak at 1400-1600 nm is due to the proximity to the detection limit of this model of instrument, which is also observed in other literature.[2]

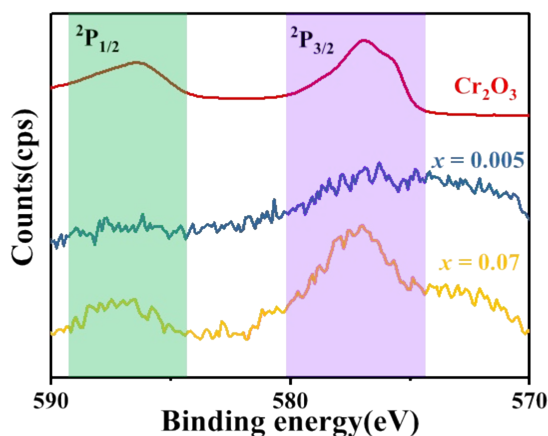

Fig. S7 High-resolution XPS spectrum of Cr 2p level.

The crystal field splitting Dq, the Racah parameter B, and the Dq/B value can be calculated by the following equation:[3]

$$10\,Dq = E(^4T_2) = E(^4T_2 \leftarrow {}^4A_2)\ \#(1)$$

$$\frac{Dq}{B} = \frac{15(\Delta E/Dq - 8)}{(\Delta E/Dq)^2 - 10(\Delta E/Dq)}\ \#(2)$$

$$\Delta E = E(^4T_1) - E(^4T_2) = E(^4T_1 \leftarrow {}^4A_2) - E(^4T_2 \leftarrow {}^4A_2)\ \#(3)$$

where $E(^4T_1 \leftarrow ^4A_2)$ and $E(^4T_2 \leftarrow ^4A_2)$ are the peak energies of the $^4T_1(^4F) \leftarrow ^4A_2$ and $^4T_2(^4F) \leftarrow ^4A_2$ transitions, respectively. As shown in **Fig. S8**, the Dq/B value of $Sc_{2-x}Si_2O_7$:$x$$Cr^{3+}$ is 2.05.

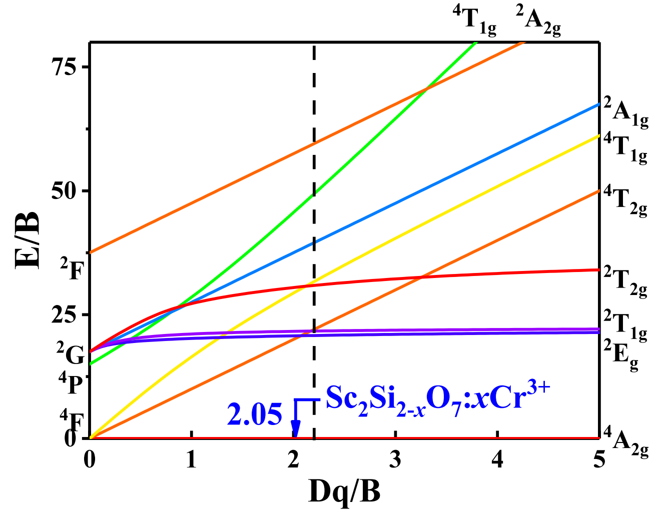

Fig. S8 Dq/B value of $Sc_{2-x}Si_2O_7$:$x$$Cr^{3+}$ and T–S energy level diagram for Cr^{3+} in the octahedral environment.

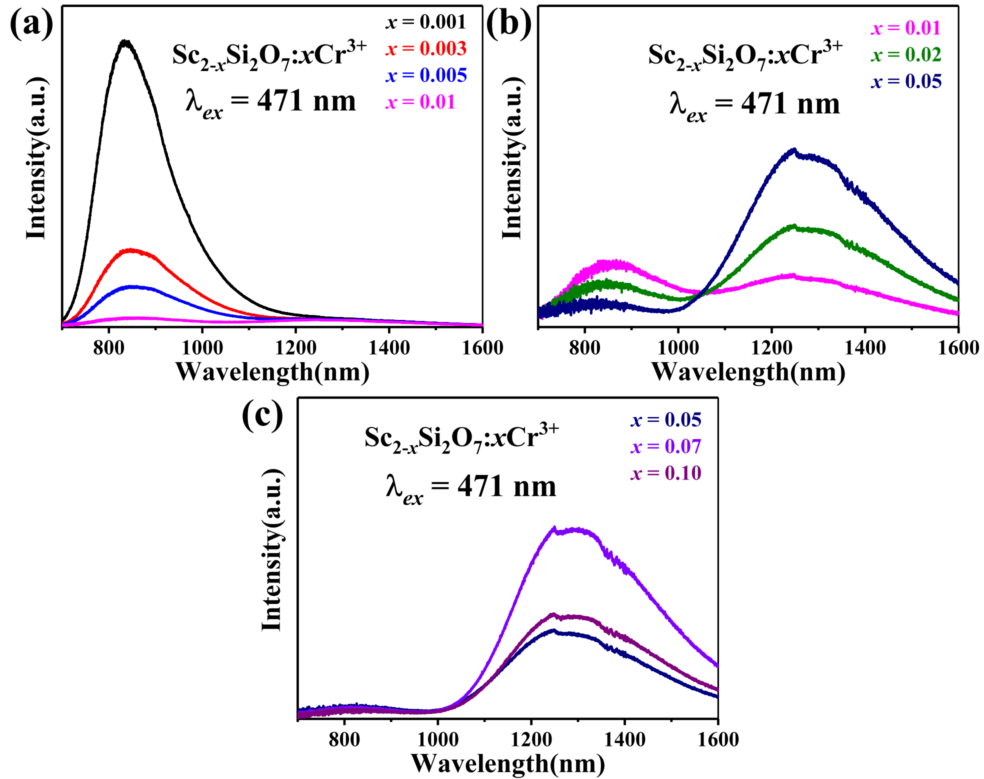

Fig. S9 PL spectra of the split concentration (a) $x = 0.001\text{-}0.01$ (b) $x = 0.01\text{-}0.05$ (c) $x = 0.05\text{-}0.10$

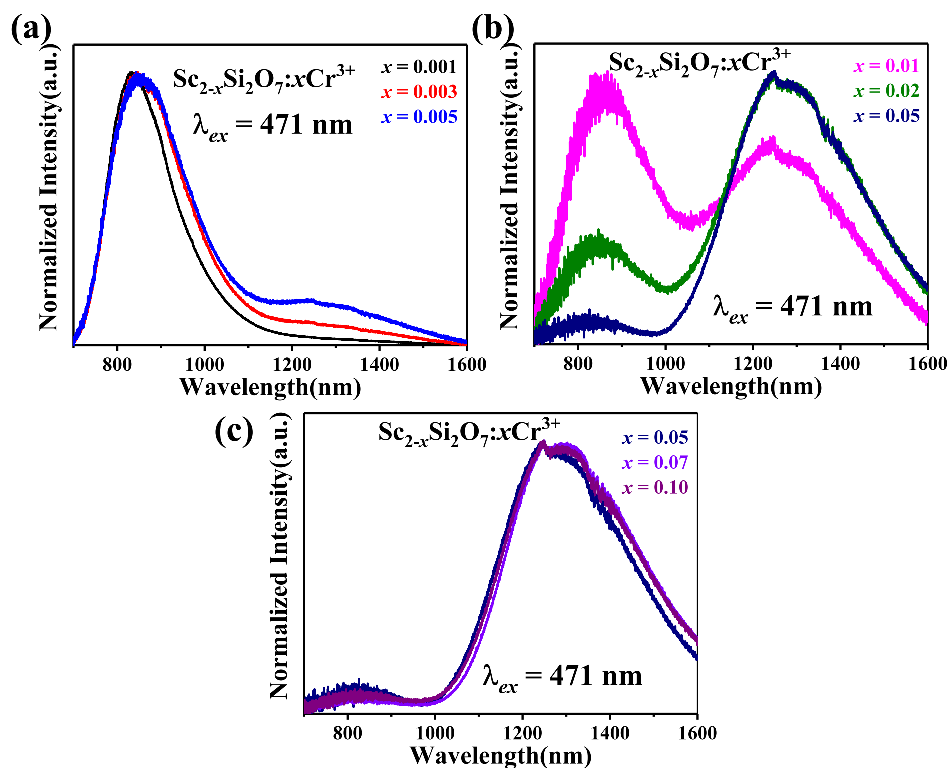

Fig. S10 PL spectra of the split concentration(Normalized) (a) $x = 0.001\text{-}0.01$ (b) $x = 0.01\text{-}0.05$ (c) $x = 0.05\text{-}0.10$

References

1 B. H. Toby and R. B. Von Dreele, *Journal of Applied Crystallography*, 2013, **46**, 544–549.

2 X. Zou, X. Wang, H. Zhang, Y. Kang, X. Yang, X. Zhang, M. S. Molokeev and B. Lei, *Chemical Engineering Journal*, 2022, **428**, 132003.

3 Q. Zhang, X. Wei, J. Zhou, B. Milićević, L. Lin, J. Huo, J. Li, H. Ni and Z. Xia, *Advanced Optical Materials*, 2023, **11**, 2300310.